Exploring information exchange between *Thesium chinense* and its host *Prunella vulgaris* through joint transcriptomic and metabolomic analysis

Anping Ding[1¶], Zengxu Xiang[1¶,*], Ruifeng Wang[1], Juan Liu[2], Wenna Meng[2], Yu Zhang[1], Guihong Chen[1], Gang Hu[2], Mingpu Tan[2*]

[1] College of Horticulture, Nanjing Agricultural University, Nanjing, Jiangsu, China

[2] College of Life Sciences, Nanjing Agricultural University, Nanjing, Jiangsu, China

Email: 2021804301@stu.njau.edu.cn (A.D.); zxxiang@njau.edu.cn (Z.X.); 2021804292@stu.njau.edu.cn (R.W.); 2021116018@stu.njau.edu.cn (J.L.); 2022116038@stu.njau.edu.cn (W.M.); 2022804334@stu.njau.edu.cn (Y.Z.); 2021104131@stu.njau.edu.cn (G.C.); hugang@njau.edu.cn (G.H.); tempo@njau.edu.cn (M.T.).

[*] Corresponding authors

E-mail: zxxiang@njau.edu.cn (Z.X.); tempo@njau.edu.cn (M.T.)

¶These authors contributed equally to this work.

Running title: Transmitted information between parasitic *Thesium chinense* and its host *Prunella vulgaris*

Abstract

Background: *Thesium chinense* known as "plant antibiotic" is a facultative root hemi-parasitic herb while *Prunella vulgaris* can serve as its host. However, the molecular mechanisms underlying the communication between *T. chinense* and its host remained largely unexplored. The aim of this study was to provide a comprehensive view of transferred metabolites and mobile mRNAs between *T. chinense* and *P. vulgaris*. Results: The wide-target metabolomic and transcriptomic analysis identified 5 transferred metabolites and 668 mobile genes between *T. chinense* and *P. vulgaris*, as well as haustoria formation related 56 metabolites and 189 genes. Furthermore, we inferred a regulatory network that might be involved in haustoria formation, and 18 genes promoting haustoria formation and 1 gene inhibiting it were identified as a consequence. There were 4 metabolites (ethylsalicylate, eriodictyol-7-O-glucoside, aromadendrin-7-O-glucoside and pruvuloside B) that are transferred from *P. vulgaris* to *T. chinense*, whereas 2-ethylpyrazine was transferred from *T. chinense* to *P. vulgaris*. Conclusions: These results suggested that there was an extensive exchange of information with *P. vulgaris* including transferred metabolites and mobile mRNAs, which might facilitate the haustoria formation and parasition of *T. chinense*.

Keywords: *T. chinense*; *P. vulgaris*; transferred metabolite; mobile gene; haustoria formation

Author summary

T. chinense known as "plant antibiotic" is a facultative root hemi-parasitic herb while *P. vulgaris* can serve as its host. Currently, the information exchange between *T. chinense* and its host

remained unknown, and a comprehensive view of transferred metabolites and mobile mRNAs between *T. chinense* and its host is critical so that appropriate chemical and genetic improvement can be used to facilitate haustoria formation and successful parasitism. Here, we employ the conjoint wide-target metabolomic and transcriptomic analysis to explore the information exchange between *T. chinense* and *P. vulgaris.* We identified 5 transferred metabolites and 668 mobile genes between *T. chinense* and *P. vulgaris*, as well as haustoria formation related 56 metabolites and 189 genes. Our study provides new insights into the complex interplay between parasite and host during parasitism.

Introduction

Parasitic plants are greatly diverse, which are currently categorized on two main bases: holoparasite and hemiparasite according to whether they are able to photosynthesis or not, and rootparasite and stemparasite according to the location of the parasitism on the host plant [1,2]. Despite their remarkable diversity, all parasitic plants share a unique specialized organ called the haustorium [3], which was described as "the essence of parasitism" [4]. During the interaction with their hosts, the haustorium exhibits dynamic changes in its functions. Early in the commensal process, the haustorium aids parasite in host attachment and invasion, and subsequently, it facilitates the uptake of nutrients, hormones and signaling molecules [5]. The resulting symplastic continuity enables macromolecules or genetic materials such as RNA to be transferred between the hosts and the parasites [6].

T. chinense is a hemiparasitic plant of the genus *Thesium* in the Santalaceae family, which is widely distributed in China, Japan, and Korea [7]. Modern pharmacological researches have proved

that *T. chinense* has diverse activities including anti-inflammation [8,9], antimicrobial effect [10–13], analgesic activity [14], antioxidant activity [15] and anti-nephropathy [16]. Moreover, *T. chinense* known as "plant antibiotic" [17] has a great deal of efficacy for the treatment of mastitis, tonsillitis, pharyngitis, pneumonia, and upper respiratory tract infections [11,18,19]. The hosts of *T. chinense* are distributed extensively in many plant families [20], including *P. vulgaris*, a perennial herb in the family Lamiaceae [21]. *T. chinense* is a root-parasitic plant, which is attached to the roots of *P. vulgaris* by the haustoria to sustain its own growth and development.

Due to their unique ways of symbiosis, the parasitic plants not only absort water [22] and nutrients from the host, but also leverage secondary metabolites, mRNA [23,24], proteins [24], and systemic signals [25,26] from their hosts. *Cistanche deserticola* utilizes its host *Haloxylon ammodendron* derived metabolites for better survival [27]. *Cuscuta* not only transmits mRNAs between different host plants [28], but also exchanges proteins with its hosts, and even proteins with the same functions can be transferred between different host plants of *Cuscuta* [29]. Parasites plant may also actively transfer phytohormones to the hosts to manipulate host physiology [25]. In recent years, the researches of *T. chinense* focused on the regulation of seed dormancy-breaking growth and development [30], in vitro anti-inflammatory and antimicrobial activity of extracts [8,11,31,32], host range and selectivity [33], and developmental reprogramming of haustoria formation [34]. In contrast, there are fewer studies on the exchange of information between *T. chinense* and host plants. Therefore, it is necessary to further investigate the molecular mechanism governing the interaction crucial for successful parasitism and the subsequent symbiosis between parasitic plants and the host.

To explore the information exchange events between *T. chinense* and *P. vulgaris*, we

conducted an integrated wide-target metabolomic and transcriptomic analysis, especially during the established parasitism relationship between *T. chinense* and its host, *P. vulgaris*. In this sutdy, 5 transferred metabolites and 668 mobile genes were identified between *T. chinense* and *P. vulgaris*, as well as haustoria formation related 56 metabolites and 189 genes. By comparing the gene expression profiles and metabolic profiles of both partners, we aim to identify key genes and metabolites involved in the establishment and maintenance of the parasitic relationship. This study not only explored the information exchange events between *T. chinense* and its host, *P. vulgaris*, but also discussed major understandings of haustoria formation and host invasion, shedding light on the complex interplay between parasite and host during parasitism.

Results

Root morphology of *T. chinense* and its host *P. vulgaris* post parasition

The root morphology of individual *T. chinense* and its host *P. vulgaris*, and the chimeric root post symbiosis were observed histologically (Fig. 1A). The result showed that there were a large number of ivory spherical haustoria at the root of *T. chinense* (Fig. 1B). Although the roots of *T. chinense* were tightly attached to the roots of *P. vulgaris*, the haustoria did not completely penetrate the roots of *P. vulgaris* (Fig. 1C), implying that the bridge between *P. vulgaris* chimera and the haustorium was undergoing changes and transmitting cargos (Fig. 1D). To explore the information exchange events between *T. chinense* and its host *P. vulgaris*, *T. chinense* chimera (THC) and *P. vulgaris* chimera (PC) from the symbiont roots, and the root counterparts of independent *T. chinense* (TH) and *P. vulgaris* (P) seedlings were collected for the subsequent

transcriptomic and metabolomic analysis.

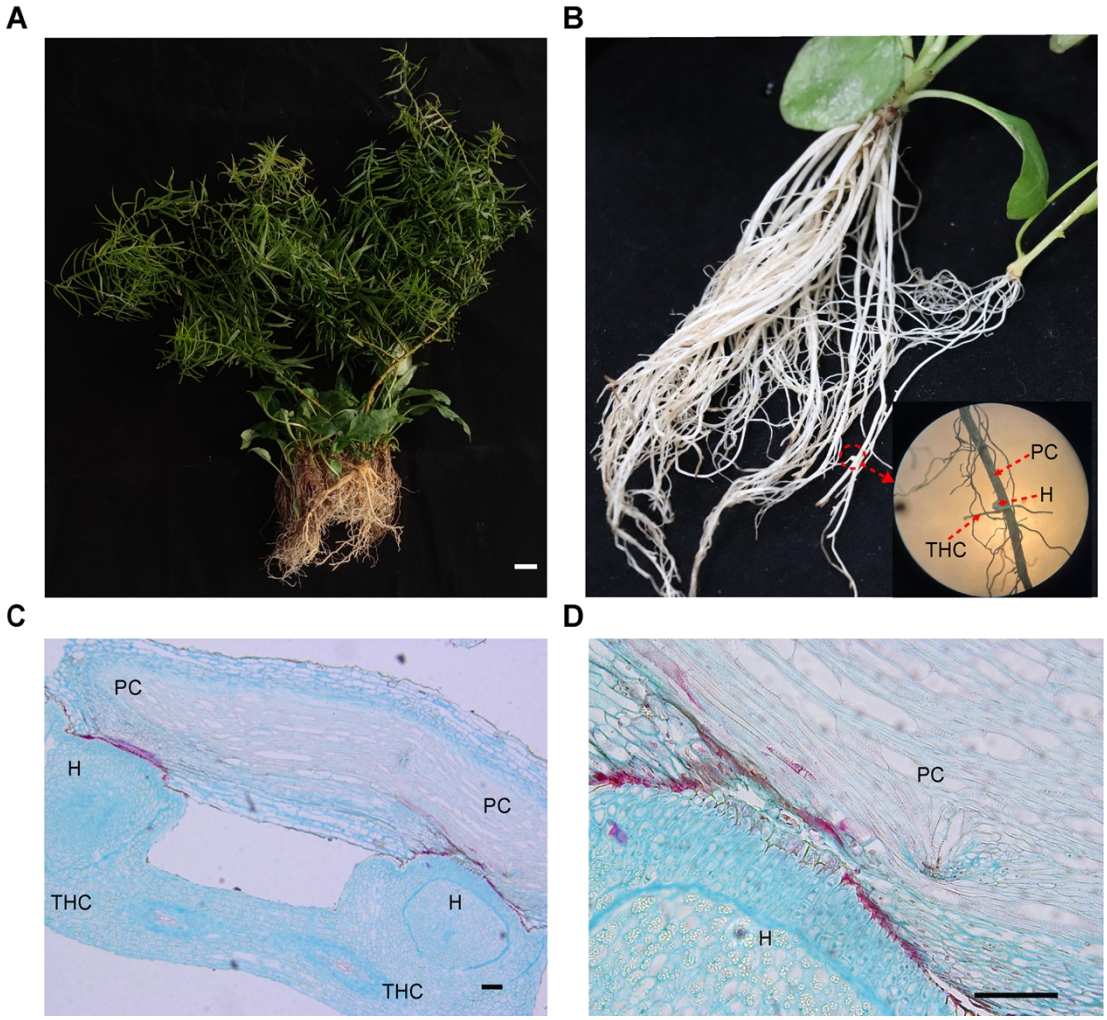

Fig. 1 Morphology of *T. chinense* and its host *P. vulgaris* chimeric root. A: *T. chinense* and its host *P. vulgaris*. B: *T. chinense* chimera is connected to its host *P. vulgaris* chimera through haustoria. C-D: Structure of *T. chinense* chimera, haustoria and *P. vulgaris* chimera. THC: *T. chinense* chimera. H: Haustorium. PC: *P. vulgaris* chimera.

Metabolomic changes in *T. chinense* and its host *P. vulgaris* post symbiosis

To identify the metabolites transferred between *T. chinense* and its host *P. vulgaris*, the wide-target metabolomic analysis was conducted. Consequently, 1,014 metabolites were identified in *T.*

117 *chinense*, *P. vulgaris* and their chimeras (Fig. 2A and S1 Table), and the PCA analysis of these
118 metabolites showed that they can be clearly separated into four clusters corresponding to the four
119 sampling groups (Fig. 2B). These results suggested significantly different pattern of metabolites
120 accumulation among TH, THC, PC, and P, emphasizing the changes caused by parasites.

121 Then the differentially accumulated metabolites (DAMs) in *T. chinense* and its host *P.*
122 *vulgaris* post symbiosis, were identified using the screening criteria of $|\log_2\text{FoldChange}| \geq 1$ and
123 VIP ≥ 1. Compared with the roots of intact *T. chinense*, 252 DAMs were identified in *T. chinense*
124 chimera, of which 75 were upregulated and 177 were downregulated (S2 Table). Compared with
125 the roots of parasition-free *P. vulgaris*, a total of 194 DAMs were identified in *P. vulgaris*
126 chimera, of which 159 were upregulated while 35 were downregulated (S3 Table). Moreover, 56
127 common DAMs were altered both in PC and THC compared to the roots of *T. chinense* and *P.*
128 *vulgaris*, therefore, these 56 DAMs can be regarded as haustoria formation related metabolites
129 (Table 1 and Fig. 2C).

130 Regarding the DAMs category, phenolic acids, amino acids and derivatives, flavonoids and
131 alkaloids accounted for more than half of the total DAMs in the TH vs THC group. Phenolic acids
132 had the highest percentage of 27.38% (Fig. 3A), and most of the phenolic acids in *T. chinense*
133 chimera showed a decreasing trend compared to *T. chinense*, but ethylsalicylate was upregulated
134 in *T. chinense* chimera. A total of 23 flavonoids were detected, and most of DAMs associated with
135 flavonoid biosynthesis including kaempferol derivatives were downregulated in *T. chinense*
136 chimera. Another notable issue is that most of the auxin biosynthesis related components,
137 including indole, 3-indolepropionic acid, and 3-indoleacrylic acid were downregulated in *T.*
138 *chinense* chimera (S2 Table).

In the P vs PC comparison group, DAMs in the category of phenolic acids, flavonoids and terpenoids accounted for 14.43%, 5.15% and 7.73%, respectively (Fig. 3B). Compared to *P. vulgaris*, ferulic acid methyl ester and p-coumaric acid methyl ester accumulated more in the *P. vulgaris* chimera, whereas the accumulation of protocatechuic acid, salicylic acid-2-O-glucoside, and arbutin was in the contrast trend. After symbiosis, the content of most flavonoids increased in *P. vulgaris* chimera. Interestingly, terpenoids (including kaurenoic acid, 18-oxoferruginol, and serratagenic acid) and jasmonic acid (JA) were all upregulated in *P. vulgaris* chimera (S3 Table).

Table 1. Differentially accumulated metabolites (DAMs) related to haustoria formation.

Compounds	CAS	Category	Type	
			THvsTHC	PvsPC
2,3,19-Trihydroxyurs-12-en-28-oic acid	-	Terpenoids	up	up
Pinfaensic acid	-	Terpenoids	up	up
N,N'-Dimethylarginine	30344-00-4	Amino acids and derivatives	up	up
N-Monomethyl-L-arginine	17035-90-4	Amino acids and derivatives	up	up
L-Isoleucyl-L-Aspartate	-	Amino acids and derivatives	up	up
L-Aspartyl-L-Phenylalanine	13433-09-5	Amino acids and derivatives	up	up
Candelabrone 12-methyl ether	-	Terpenoids	up	up
19-Hydroxyursolic acid	-	Terpenoids	up	up
Homoarginine	156-86-5	Amino acids and derivatives	up	up
NG,NG-Dimethyl-L-arginine	30315-93-6	Amino acids and derivatives	up	up
2-Deoxyribose-1-phosphate	17210-42-3	Nucleotides and derivatives	up	up
6'-O-Feruloyl-D-sucrose	118230-77-6	Phenolic acids	up	up
Jasmonic acid	77026-92-7	Organic acids	up	up
2-Acetoxymethyl-anthraquinone	-	Quinones	up	up
Propyl 4-hydroxybenzoate	94-13-3	Phenolic acids	up	up
5-hydroxy-1-phenyl-7-3-heptanone	-	Others	up	up
2,2-Dimethylsuccinic acid	597-43-3	Organic acids	up	up
L-Tartaric acid	87-69-4	Organic acids	up	down
Tachioside	109194-60-7	Phenolic acids	down	down
Isotachioside	31427-08-4	Phenolic acids	down	down
1-O-Salicyloyl-β-D-glucose	60517-74-0	Phenolic acids	down	down
Salicylic acid-2-O-glucoside	10366-91-3	Phenolic acids	down	down
p-Hydroxypheny-β-D-allopyranoside	-	Phenolic acids	down	down
Arbutin	497-76-7	Phenolic acids	down	down
Sinapoyl malate	92344-58-6	Phenolic acids	down	down

2-O-Caffeoylglucaric Acid	-	Phenolic acids	down	down
Oleic acid	112-80-1	Lipids	down	down
N-Methyl-Trans-4-Hydroxy-L-Proline	4252-82-8	Amino acids and derivatives	down	down
2,6-Dimethoxy-4-hydroxyphenol-1-O-ß-D-glucopyranoside	-	Others	down	down
Methoxyindoleacetic acid	3471-31-6	Alkaloids	down	up
Tryptamine	61-54-1	Alkaloids	down	up
L-Tryptophan	73-22-3	Amino acids and derivatives	down	up
3-Indoleacetonitrile	771-51-7	Alkaloids	down	up
1-Methoxy-indole-3-acetamide	-	Alkaloids	down	up
Indole	120-72-9	Alkaloids	down	up
3-Indolepropionic acid	830-96-6	Alkaloids	down	up
3-Indoleacrylic acid	1204-06-4	Alkaloids	down	up
γ-glutamylmethionine	17663-87-5	Amino acids and derivatives	down	up
2-Aminoethanesulfonic acid	107-35-7	Organic acids	down	up
p-Coumaric acid methyl ester	19367-38-5	Phenolic acids	down	up
Roseoside	54835-70-0	Others	down	up
Isoquinoline	119-65-3	Alkaloids	down	up
4-caffeoylshikimic acid	-	Phenolic acids	down	up
L-Histidine	71-00-1	Amino acids and derivatives	down	up
Phlorizin	60-81-1	Flavonoids	down	up
3,4-Methylenedioxy cinnamyl alcohol	58095-76-4	Lignans and Coumarins	down	up
Kaurenoic Acid	6730-83-2	Terpenoids	down	up
LysoPC 15:0	108273-89-8	Lipids	down	up
Melibiose	585-99-9	Others	down	up
3-amino-2-naphthoic acid	-	Alkaloids	down	up
L-Lysine-Butanoic Acid	80407-71-2	Amino acids and derivatives	down	up
cyclo-(Gly-Phe)	10125-07-2	Amino acids and derivatives	down	up
Trans-Citridic acid	4023-65-8	Organic acids	down	up
1-O-Sinapoyl-β-D-glucose	-	Phenolic acids	down	up
Linarin	480-36-4	Flavonoids	down	up
Syringaresinol-4'-O-glucoside	7374-79-0	Lignans and Coumarins	down	up

147 CAS: Chemical Abstracts Service registry number. TH: *T. chinense*. THC: *T. chinense* chimera.

148 PC: *P. vulgaris* chimera. P: *P. vulgaris*.

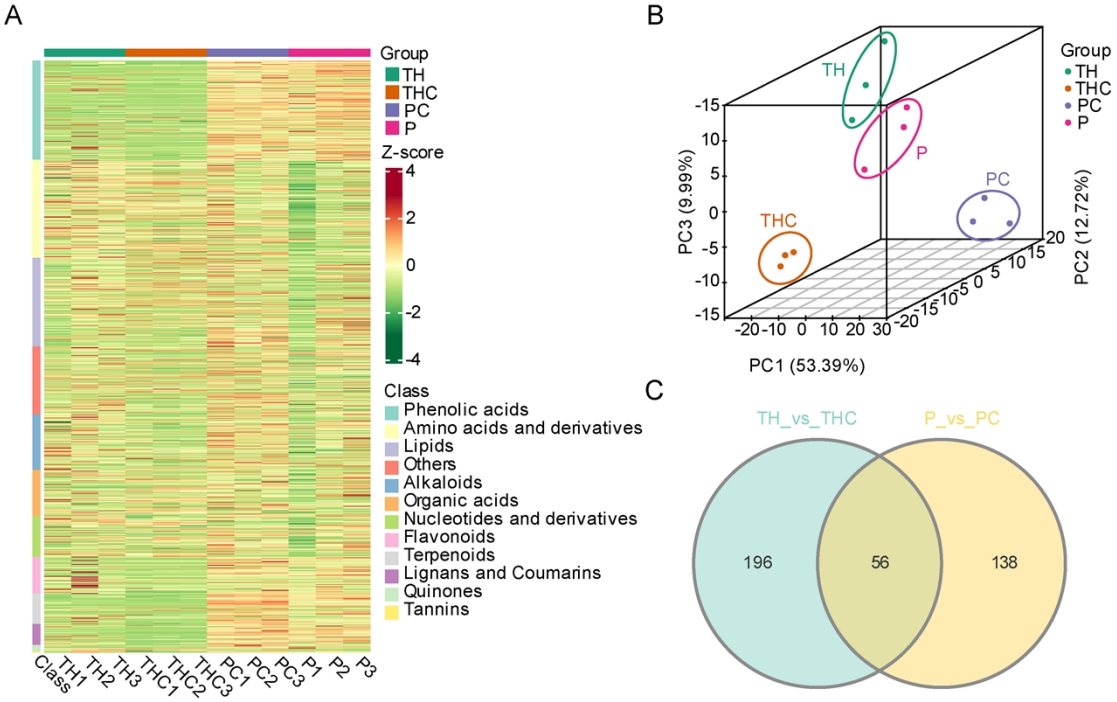

149 **Fig. 2 The metabolomic analysis of *T. chinense* and its host *P. vulgaris* post symbiosis.** A:

150 Heat map visualization of metabolites in *T. chinense*, *P. vulgaris* roots and their chimera. B: PCA

151 analysis of metabolites in *T. chinense*, *P. vulgaris* roots and their chimera. C: Venn diagrams

152 revealing the relationship of differentially accumulated metabolites (DAMs) in *T. chinense*

153 chimera and its host *P. vulgaris* chimera. TH: *T. chinense*. THC: *T. chinense* chimera. PC: *P.*

154 *vulgaris* chimera. P: *P. vulgaris*.

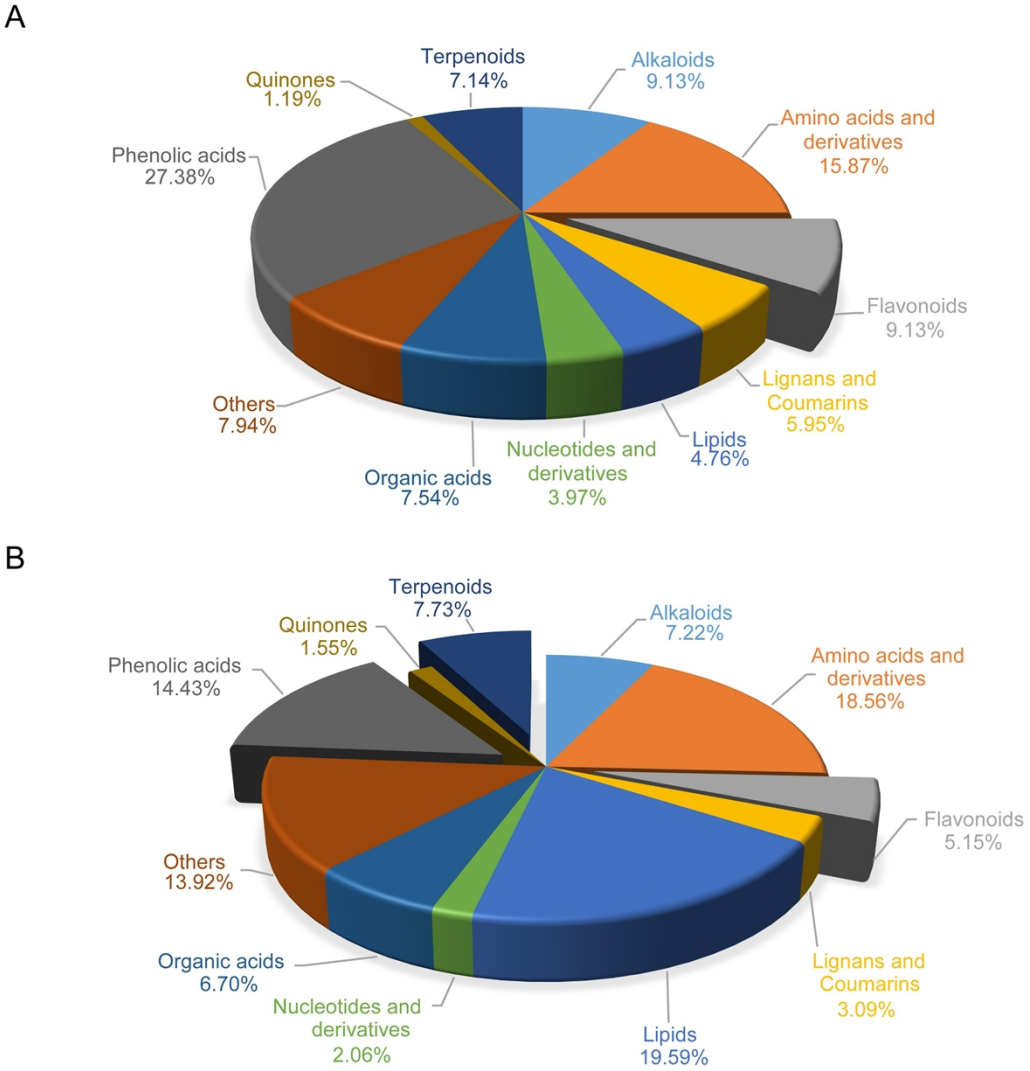

155 **Fig. 3 The proportion of differentially accumulated metabolites (DAMs) category in *T.***

156 ***chinense* chimera and its host *P. vulgaris* chimera.** A: TH vs THC. B: P vs PC. TH: *T. chinense*.

157 THC: *T. chinense* chimera. PC: *P. vulgaris* chimera. P: *P. vulgaris*.

158 The exchanges of metabolites between *T. chinense* and its
159 host *P. vulgaris* during parasitism

160 To explore the information exchange between *T. chinense* and its host *P. vulgaris*, the

161 accumulation pattern of metabolites in the four groups (TH, THC, PC, and P) was compared.

162 Consequently, those metabolites not detected in TH or P but accumulated in other three samples

were defined as transferred metabolites. As a result, 5 transferred metabolites (ethylsalicylate, eriodictyol-7-O-glucoside, aromadendrin-7-O-glucoside, pruvuloside B, 2-ethylpyrazine) were identified (Table 2). Particularly pruvuloside B, a characteristic component of *P. vulgaris*, was detected in PC, P and THC, however it was not found in TH roots, suggesting a transfer of this metabolite from *P. vulgaris* chimera to *T. chinense* chimera (host→parasite direction). Similar host→parasite mobile metabolites include ethylsalicylate, eriodictyol-7-O-glucoside, and aromadendrin-7-O-glucoside. By Contrast, 2-ethylpyrazine was presented in TH, THC, and PC but not in P roots, indicating that this metabolite was transferred from *T. chinense* chimera to *P. vulgaris* chimera (parasite→host direction).

Regarding the haustoria formation related hormones, the auxin biosynthesis related components accumulated significantly more in PC, whereas the opposite was true in THC. Jasmonic acid (JA) was upregulated in both THC and PC. Moreover, another 16 metabolites were also synchronized upregulated in both chimeras groups, and these metabolites can be considered as promoting haustoria formation. Conversely, 11 metabolites downregulated in both chimeras groups may inhibit haustoria formation (Table 1 and S4 Table).

Table 2. The transferred metabolites between *T. chinense* and its host *P. vulgaris*.

Compounds	CAS	Category	TH	THC	PC	P
Ethylsalicylate	118-61-6	Phenolic acids	-	35397	500949	542212
Eriodictyol-7-O-glucoside	38965-51-4	Flavonoids	-	29411	3851867	4694065
Aromadendrin-7-O-glucoside	28189-90-4	Flavonoids	-	113418	1191540	604233
Pruvuloside B	-	Terpenoids	-	1789	54923	40759
2-Ethylpyrazine	13925-00-3	Alkaloids	49686	43058	78849	-

CAS: Chemical Abstracts Service registry number. TH: *T. chinense*. THC: *T. chinense* chimera. PC: *P. vulgaris* chimera. P: *P. vulgaris*.

Transcriptomic changes in *T. chinense* and its host *P. vulgaris* post symbiosis

Besides the metabolomic fluctuation, the parasitism of *T. chinense* also caused significant transcriptomic changes. To address this issue, transcriptomic profiling of the root samples of TH, THC, PC and P were conducted. Then a stringent cutoff ($|\log_2 FoldChange| \geq 1$ with the adjusted p-value padj < 0.05) was used to identify differentially expressed genes (DEGs) in *T. chinense*, *P. vulgaris* and their chimeras post parasition. Consequently, 11640 and 8705 DEGs were identified in the comparison of TH vs THC (S5 Table) and P vs PC (S6 Table), respectively.

To infer the biological functions of DEGs of *T. chinense* and its host *P. vulgaris* post symbiosis, the GO and KEGG enrichment analysis of DEGs were performed. Regarding the DEGs in TH vs THC group, the GO entries and proportions with the most significant enrichment in biological process, cellular component, and molecular function were photosynthesis/light reaction, photosystem and hydrolase activity/hydrolyzing N-glycosyl compounds, respectively (Fig. 4A), while the three most significant counterparts in P vs PC group were amino acid transport, ER body, and organic acid binding (Fig. 4B). The KEGG enriched pathways of DEGs in TH vs THC and P vs PC were similar, both including phenylpropanoid biosynthesis, flavonoid biosynthesis and plant hormone signal transduction. In addition, the DEGs in the TH vs THC group were also highly enriched in fructose and mannose metabolism, vitamin B6 metabolism and photosynthesis-antenna proteins (Fig. 4C). However, the highly represented pathways of DEGs in P vs PC were plant-pathogen interaction and MAPK signaling pathway-plant (Fig. 4D).

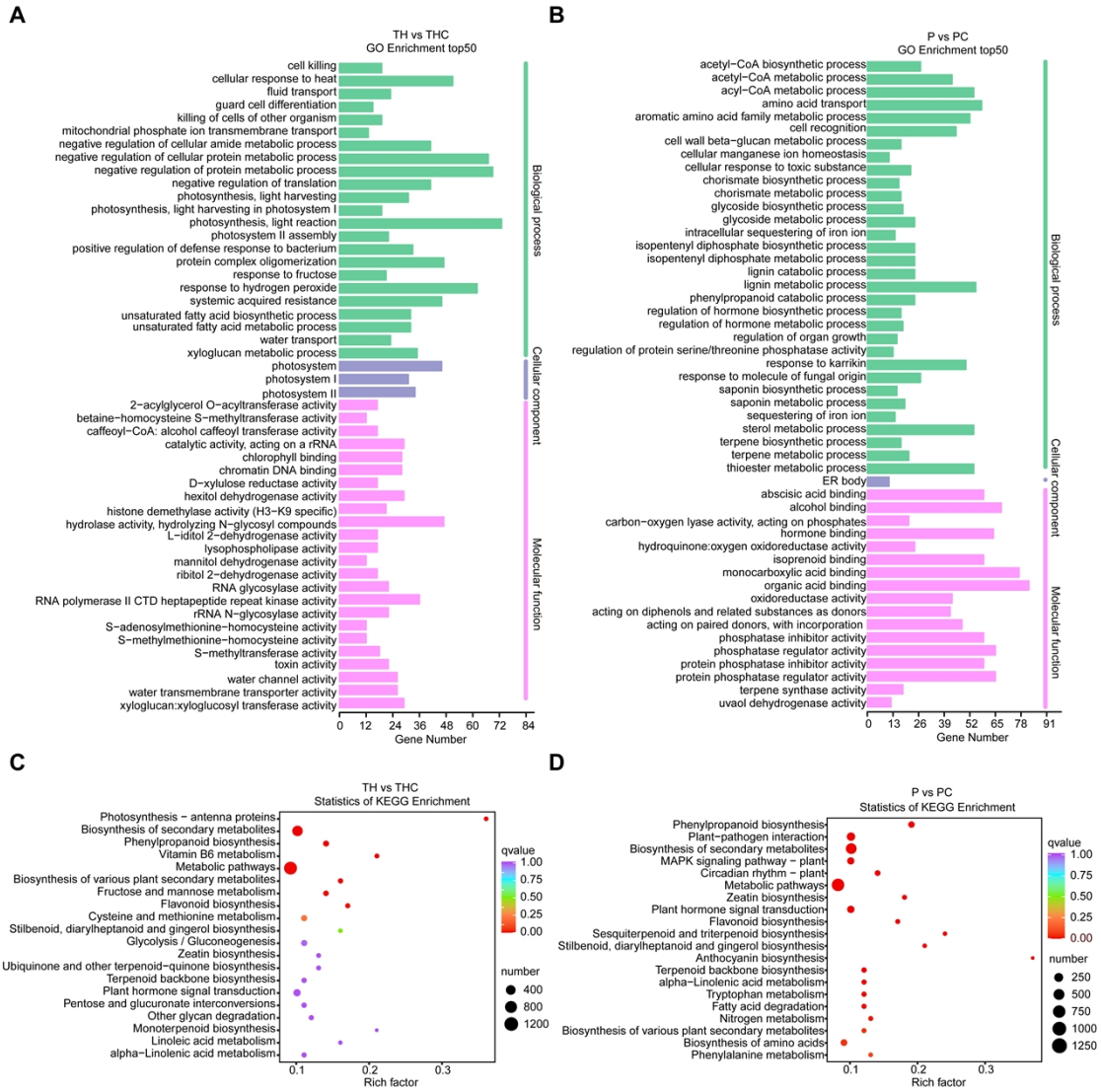

Fig. 4 The enrichment analysis of DEGs based on GO terms and KEGG pathways. A: GO terms of DEGs in TH vs THC. B: GO terms of DEGs in P vs PC. C: KEGG pathway analysis of DEGs in TH vs THC. D: KEGG pathway analysis of DEGs in P vs PC. TH: *T. chinense*. THC: *T. chinense* chimera. PC: *P. vulgaris* chimera. P: *P. vulgaris*.

The mobile genes between *T. chinense* and its host P. *vulgaris*

To further explore the information exchange events of genes between *T. chinense* chimera and its host *P. vulgaris* chimera at molecular level, we combined RNA-sequencing and stepwise

209 bioinformatic classification to identify mobile transcripts between parasite plant and its host.

210 Consequently, 383 unigenes are most probably of *T. chinense* origin because of their absence
211 only in P, and they are mobile genes transferred from *T. chinense* chimera to *P. vulgaris* chimera
212 (Fig. 5 and S7 Table). The putative function classes of these parasite→host mobile genes were
213 carbon metabolism, terpenoid biosynthesis, plant hormone signal transduction, ABC transporters,
214 and plant-pathogen interaction (Table 3). Similarly, 285 unigenes are mobile genes transferred
215 from *P. vulgaris* chimera to *T. chinense* chimera (Fig. 5 and S8 Table). Among them, the
216 pathways these host→parasite mobile genes were fatty acid, steroid biosynthesis and plant-
217 pathogen interaction (Table 3). Moreover, 189 (TH-exclusive and P-exclusive) common unigenes
218 were finally retrieved from THC and PC (Fig. 5 and S9 Table), and these genes might be closely
219 related to haustoria formation.

220 **Table 3. The mobile genes between *T. chinense* and *P. vulgaris*.**

Transcript-ID	Homolog	Annotation
From *T. chinense* to *P. vulgaris* (parasite→host)		
	Glycolysis / Gluconeogenesis	
Cluster-25895.9	G6PI_SPIOL	Glucose-6-phosphate isomerase, cytosolic
Cluster-18005.2	TPIS_COPJA	Triosephosphate isomerase, cytosolic
Cluster-75330.1	AL2B4_ARATH	Aldehyde dehydrogenase family 2 member B4, mitochondrial
Cluster-79797.9	AL3H1_ARATH	Aldehyde dehydrogenase family 3 member H1
Cluster-37316.1	G3PC_MAGLI	Glyceraldehyde-3-phosphate dehydrogenase, cytosolic
Cluster-20103.8	G3PC_SINAL	Glyceraldehyde-3-phosphate dehydrogenase
Cluster-25297.1	PGKY3_ARATH	Phosphoglycerate kinase 3, cytosolic
Cluster-28101.6	PDC1_PEA	Pyruvate decarboxylase 1
Cluster-22031.6	ENO_RICCO	Enolase
	Citrate cycle (TCA cycle)	
Cluster-28895.3	IDHP_MEDSA	Isocitrate dehydrogenase [NADP], chloroplastic
Cluster-31044.5	CISY_CITMA	Citrate synthase, mitochondrial
	Pentose phosphate pathway	
Cluster-24281.8	ACLA1_ARATH	ATP-citrate synthase alpha chain protein 1
Cluster-25801.6	ACLB2_ARATH	ATP-citrate synthase beta chain protein 2
Cluster-28148.0	6PGD2_ARATH	6-phosphogluconate dehydrogenase, decarboxylating 2
Cluster-11481.5	G6PD_SOLTU	Glucose-6-phosphate 1-dehydrogenase, cytoplasmic isoform
Cluster-28148.0	6PGD2_ARATH	6-phosphogluconate dehydrogenase, decarboxylating 2

Pentose and glucuronate interconversions		
Cluster-6105.3	DHSO_ARATH	Sorbitol dehydrogenase
Cluster-11040.0	UGDH1_SOYBN	UDP-glucose 6-dehydrogenase 1
Cluster-29129.3	PME1_CITSI	Pectinesterase 1
Cluster-23797.2	PME3_PHAVU	Pectinesterase 3
Fructose and mannose metabolism		
Cluster-3537.6	SCRK4_ARATH	Probable fructokinase-4
Cluster-27814.3	GMPP1_ARATH	Mannose-1-phosphate guanylyltransferase 1
Starch and sucrose metabolism		
Cluster-21805.9	E1314_ARATH	Glucan endo-1,3-beta-glucosidase 14
Cluster-11525.7	BAM1_ARATH	Beta-amylase 1, chloroplastic
Cluster-10599.7	TPS9_ARATH	Probable alpha,alpha-trehalose-phosphate synthase
Cluster-18065.7	TPPA_ARATH	Trehalose-phosphate phosphatase A
Amino sugar and nucleotide sugar metabolism		
Cluster-30415.1	CHLY_HEVBR	Hevamine-A
Cluster-18226.7	AXS2_ARATH	UDP-D-apiose/UDP-D-xylose synthase 2
Cluster-33081.2	RGP2_SOLTU	Probable UDP-arabinopyranose mutase 2
Cluster-9320.1	WIN2_SOLTU	Wound-induced protein WIN2
Ubiquinone and other terpenoid-quinone biosynthesis		
Cluster-28306.9	TCMO_CATRO	Trans-cinnamate 4-monooxygenase
Cluster-28297.0	4CL2_TOBAC	4-coumarate--CoA ligase 2
Cluster-28297.1	CCL1_HUMLU	4-coumarate--CoA ligase CCL1
Terpenoid backbone biosynthesis		
Cluster-29141.3	HMDH_CAMAC	3-hydroxy-3-methylglutaryl-coenzyme A reductase
Cluster-23422.25	MVD2_PANGI	Diphosphomevalonate decarboxylase 2
Cluster-27980.9	FPS_PANGI	Farnesyl pyrophosphate synthase
Cluster-27143.0	FPPS1_LUPAL	Farnesyl pyrophosphate synthase 1
Monoterpenoid biosynthesis		
Cluster-31749.9	MTPS1_SANAL	(+)-alpha-terpineol synthase
Phenylpropanoid biosynthesis		
Cluster-31985.1	MTDH_FRAAN	Probable mannitol dehydrogenase
Cluster-24856.0	C7A12_PANGI	Cytochrome P450 CYP736A12
Cluster-29613.0	CCR1_PETHY	Cinnamoyl-CoA reductase 1
Cluster-29531.6	NAC2_ARATH	NAC domain-containing protein 2
Cluster-29531.7	PER17_ARATH	Peroxidase 17
Cluster-27322.0	PER70_MAIZE	Peroxidase 70
Cluster-12091.2	PER42_ARATH	Peroxidase 42
Cluster-26662.0	PER51_ARATH	Peroxidase 51
Cluster-28518.6	CSE_ARATH	Caffeoylshikimate esterase
Cluster-30518.0	MTDH_FRAAN	Probable mannitol dehydrogenase
Biosynthesis of unsaturated fatty acids		
Cluster-73680.4	FAD3C_HELAN	sn-2 acyl-lipid omega-3 desaturase, chloroplastic
Cluster-29294.2	FAD2_VERFO	Delta(12)-fatty-acid desaturase FAD2
ABC transporters		
Cluster-3645.1	AB11B_ARATH	ABC transporter B family member 11
Cluster-12705.5	PDR1_TOBAC	Pleiotropic drug resistance protein 1
Cluster-27251.8	AB36G_ARATH	ABC transporter G family member 36
Cluster-29306.8	PDR3_TOBAC	Pleiotropic drug resistance protein 3
Plant hormone signal transduction		
Cluster-18151.0	AX22D_VIGRR	Auxin-induced protein 22D
Cluster-24298.5	SCL13_ARATH	Scarecrow-like protein 13
Cluster-28782.6	CIGR1_ORYSJ	Chitin-inducible gibberellin-responsive protein 1
Cluster-28424.0	TIF6B_ARATH	Protein TIFY 6B
Plant-pathogen interaction		
Cluster-6241.9	CDPK5_ARATH	Calcium-dependent protein kinase 5
Cluster-14013.8	CML3_ARATH	Calmodulin-like protein 3
Cluster-28129.4	PBL21_ARATH	Probable serine/threonine-protein kinase PBL21

Cluster-26905.2	CDPKW_ARATH	Calcium-dependent protein kinase 32
Cluster-23080.2	WAKLQ_ARATH	Wall-associated receptor kinase-like 20
Cluster-28681.0	FERON_ARATH	Receptor-like protein kinase FERONIA
From *P. vulgaris* to *T. chinense* (host→parasite)		
Fatty acid biosynthesis		
Cluster-90475.4	AAE13_ARATH	Malonate--CoA ligase
Cluster-70419.0	FABG_CUPLA	3-oxoacyl-[acyl-carrier-protein] reductase, chloroplastic
Steroid biosynthesis		
Cluster-79386.0	LIP2_ARATH	Triacylglycerol lipase 2
Glycolysis / Gluconeogenesis		
Cluster-86076.2	ALF_SPIOL	Fructose-bisphosphate aldolase, cytoplasmic isozyme
Cluster-91757.1	ENO_SOLLC	Enolase
Flavonoid biosynthesis		
Cluster-74300.0	DFRA_GERHY	Dihydroflavonol 4-reductase
Plant-pathogen interaction		
Cluster-85370.1	EFTU_CYAM1	Elongation factor Tu, chloroplastic
Cluster-77229.1	CDPKT_ORYSJ	Calcium-dependent protein kinase 29
Amino sugar and nucleotide sugar metabolism		
Cluster-46671.4	RHM3_ARATH	Trifunctional UDP-glucose 4,6-dehydratase RHM3
Nitrogen metabolism		
Cluster-89377.0	CYNS_PHYPA	Cyanate hydratase

TH: *T. chinense*. THC: *T. chinense* chimera. PC: *P. vulgaris* chimera. P: *P. vulgaris*.

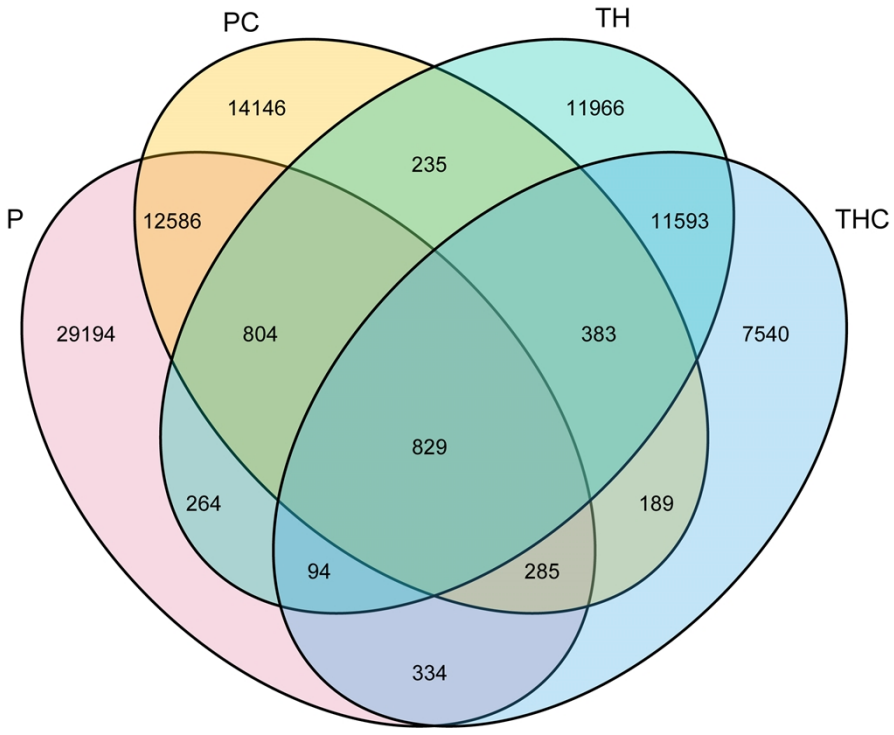

Fig. 5 Venn diagrams showing common and unique sets of transcripts in *T. chinense* and its host *P. vulgaris* following parasition. TH: *T. chinense*. THC: *T. chinense* chimera. PC: *P. vulgaris* chimera. P: *P. vulgaris*.

The conjoint analysis of genes and metabolites related to haustoria formation

To integrate the metabolome and transcriptome analysis, we performed canonical correlation analysis using the Pearson correlation coefficient (PCC) to show the dynamic changes in *T. chinense* and its host *P. vulgaris* post symbiosis. To systematically understand the metabolite-gene relationships ascribed to haustoria formation, we constructed the metabolite-gene network map with the threshold of |coefficient| > 0.8 (S10 Table). Out of the 189 genes linked to haustoria synthesis, 77 genes (Table 4) were carefully selected based on correlation with metabolites (DAMs related to haustoria formation). Subsequently, this narrowed down the search to 19 genes that were further analyzed for the network map.

The network map indicated that 18 genes upregulated in both THC and PC chimeras such as Peptide methionine sulfoxide reductase B5, Caffeoylshikimate esterase, UDP-glycosyltransferase 73D1, Expansin-like B1, Endochitinase and proteasome inhibitor were negatively correlated with the downregulated metabolites (Isotachioside, Tachioside, 1-O-Salicyloyl-β-D-glucose, Salicylic acid-2-O-glucoside, p-Hydroxypheny-β-D-allopyranoside, Oleic acid, Arbutin, 2,6-Dimethoxy-4-hydroxyphenol-1-O-ß-D-glucopyranoside) in both chimeras post symbiosis, and these 18 genes might be involve in haustorium formation (Fig. 6). Conversely, Protein phosphate-induced 1 downregulated in both THC and PC chimeras (Table 4) was negatively correlated with the upregulated metabolites (2,3,19-Trihydroxyurs-12-en-28-oic acid, Pinfaensic acid, 19-Hydroxyursolic acid, Jasmonic acid, 5-hydroxy-1-phenyl-7-3-heptanone) post symbiosis, and this gene might inhibit haustoria formation (Fig. 6).

Table 4. The genes correlated with haustoria formation related metabolites.

Transcript-ID	Homolog	Annotation
Glycolysis / Gluconeogenesis		
Cluster-20103.7	G3PC2_ARATH	Glyceraldehyde-3-phosphate dehydrogenase GAPC2, cytosolic
Cluster-57026.3	ODPB1_ORYSJ	Pyruvate dehydrogenase E1 component subunit beta-1
Cluster-80277.4	G3PC_GINBI	Glyceraldehyde-3-phosphate dehydrogenase, cytosolic
Arginine and proline metabolism		
Cluster-15047.1	SPE1_PEA	Arginine decarboxylase
Cluster-85585.19	P4H8_ARATH	Probable prolyl 4-hydroxylase 8
Terpenoid backbone biosynthesis		
Cluster-27980.8	FPPS1_LUPAL	Farnesyl pyrophosphate synthase 1
Cluster-59944.3	HMDH2_ARATH	3-hydroxy-3-methylglutaryl-coenzyme A reductase 2
Phenylpropanoid biosynthesis		
Cluster-28808.1	BBE21_ARATH	Berberine bridge enzyme-like 21
Cluster-29448.5	CSE_ARATH	Caffeoylshikimate esterase
Cluster-31390.0	CASL1_CANSA	Cannabidiolic acid synthase-like 1
Ribosome		
Cluster-28869.1	RL72_ARATH	60S ribosomal protein L7-2
Cluster-25493.2	RL72_ARATH	60S ribosomal protein L7-2
Cluster-25988.1	RL262_ARATH	60S ribosomal protein L26-2
Cluster-27350.3	RL3_ORYSJ	60S ribosomal protein L3
Ubiquitin mediated proteolysis		
Cluster-25098.3	PUB27_ARATH	U-box domain-containing protein 27
Cluster-31549.63	UBIQP_LINUS	Polyubiquitin
Plant-pathogen interaction		
Cluster-26011.1	CRK7_ARATH	Cysteine-rich receptor-like protein kinase 7
Cluster-27341.1	CML35_ARATH	Probable calcium-binding protein CML35
Cluster-61551.0	SGT1A_ARATH	Protein SGT1 homolog A
Oxidative phosphorylation		
Cluster-71915.3	VATB2_HORVU	V-type proton ATPase subunit B 2
Phosphonate and phosphinate metabolism		
Cluster-88881.1	PECT1_ARATH	Ethanolamine-phosphate cytidylyltransferase
Glutathione metabolism		
Cluster-20986.5	GSTF_HYOMU	Glutathione S-transferase

Starch and sucrose metabolism		
Cluster-18065.6	TPPG_ARATH	Probable trehalose-phosphate phosphatase G
Amino sugar and nucleotide sugar metabolism		
Cluster-40689.0	CHIT_PERAE	Endochitinase
Flavone and flavonol biosynthesis		
Cluster-26035.2	U73D1_ARATH	UDP-glycosyltransferase 73D1
mRNA surveillance pathway		
Cluster-35902.2	PABP2_ARATH	Polyadenylate-binding protein 2
RNA degradation		
Cluster-37206.1	CAF1K_ARATH	Probable CCR4-associated factor 1 homolog 11
Proteasome		
Cluster-23847.9	PSMF1_ARATH	Probable proteasome inhibitor
Protein processing in endoplasmic reticulum		
Cluster-25717.1	SSRA_ARATH	Translocon-associated protein subunit alpha
Endocytosis		
Cluster-42289.8	GNL1_ARATH	guanine-nucleotide exchange factor GNL1
Others		
Cluster-25215.6	EP1L4_ARATH	EP1-like glycoprotein 4
Cluster-26009.1	FB119_ARATH	F-box protein At2g27310
Cluster-26468.1	ERLL1_ARATH	pEARLI1-like lipid transfer protein 1
Cluster-27579.1	EXLB1_ARATH	Expansin-like B1
Cluster-27790.5	LHT1_ARATH	Lysine histidine transporter 1
Cluster-28144.0	CAES_ARATH	Probable carbohydrate esterase At4g34215
Cluster-28520.1	DUF4228	Domain of unknown function
Cluster-29252.2	RICI_RICCO	Contains: Ricin A chain
Cluster-29998.1	LEA14_GOSHI	Late embryogenesis abundant protein Lea14-A
Cluster-31749.0	MSRB5_ORYSJ	Peptide methionine sulfoxide reductase B5
Cluster-33686.3	Dehydrin	Dehydrin
Cluster-25224.2	Proline-rich	Proline-rich nuclear receptor coactivator motif
Cluster-28098.16	1433D_SOYBN	14-3-3-like protein D
Cluster-28199.1	ESSS	ESSS subunit of NADH:ubiquinone oxidoreductase
Cluster-28203.4	GILP_ARATH	GSH-induced LITAF domain protein
Cluster-2905.1	ALPL_ARATH	Protein ALP1-like
Cluster-29223.2	MSK3_MEDSA	Glycogen synthase kinase-3 homolog MsK-3

Cluster-30052.1	PHI1_TOBAC	Protein phosphate-induced 1
Cluster-37697.0	TCTP_ELAGV	Translationally-controlled tumor protein homolog
Cluster-23641.1	XTH23_ARATH	Probable xyloglucan endotransglucosylase/hydrolase protein 23
Cluster-43786.3	Lipoprotein	Lipoprotein amino terminal region
Cluster-26673.1	AMT11_SOLLC	Ammonium transporter 1 member 1
Cluster-42715.9	Prolyl	Prolyl oligopeptidase, N-terminal beta-propeller domain
Cluster-44192.13	Calponin	Calponin homology domain
Cluster-44345.9	MOCOS_ARATH	Molybdenum cofactor sulfurase
Cluster-51204.11	SRP40,	SRP40, C-terminal domain
Cluster-55729.8	Collagen	Collagen triple helix repeat
Cluster-57164.2	BTB/POZ	BTB/POZ domain
Cluster-59410.2	FLYWCH	FLYWCH zinc finger domain
Cluster-62702.5	Tudor	Tudor domain
Cluster-65349.0	MYO6_ARATH	Myosin-6
Cluster-67318.0	MHX_ARAHH	Magnesium/proton exchanger
Cluster-75878.0	SURF4	SURF4 family
Cluster-78995.0	IWS1_ARATH	Protein IWS1 homolog 1
Cluster-79820.0	CPSF2_ARATH	Cleavage and polyadenylation specificity factor subunit 2
Cluster-80491.0	MEL1_ORYSJ	Protein argonaute MEL1
Cluster-80983.2	Intermediate	Intermediate filament protein
Cluster-85779.4	Lung	Lung seven transmembrane receptor
Cluster-86623.13	Nematode	Nematode polyprotein allergen ABA-1
Cluster-88623.7	KH	KH domain
Cluster-89064.2	CATB3_ARATH	Cathepsin B-like protease 3
Cluster-89458.6	BOB1_ARATH	Protein BOBBER 1
Cluster-91151.5	CATB2_ARATH	Cathepsin B-like protease 2
Cluster-91151.7	CATB2_ARATH	Cathepsin B-like protease 2
Cluster-92130.0	ICO5D_LIMDO	Icosanoyl-CoA 5-desaturase
Cluster-92539.3	TCPQ_ARATH	T-complex protein 1 subunit theta
Cluster-30642.1	ACT1_ORYSI	Actin-1

247 TH: *T. chinense*. THC: *T. chinense* chimera. PC: *P. vulgaris* chimera. P: *P. vulgaris*.

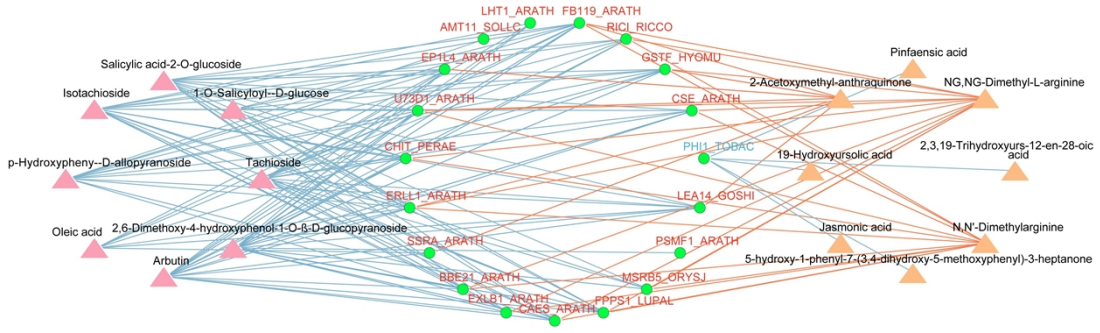

Fig. 6 The network of metabolites and genes related to haustoria formation. Genes in the green ellipse. The upregulated genes in both THC and PC chimeras were in red font and the downregulated in blue font. Metabolites downregulated in both THC and PC are in the pink triangle and metabolites upregulated in both THC and PC are in the orange triangle. For the connection between genes and metabolites, red lines indicate the positive correlation while blue lines indicate the negative correlation. The altered pattern and annotation of haustoria formation related metabolites or genes are given in S10 Table.

Discussion

T. chinense is a medically important plant that invades its host plant through the haustoria and hijacks water, nutrients, DNA, mRNA, proteins needed to sustain its own growth and development. The essence of parasite plants' life habits is to establish parasitic relationships with their host [35]. However, to date, there has been few studies on the information exchange between *T. chinense* and its host. Therefore, this study aims to explore the changes in the metabolome and transcriptome of *T. chinense* and its host *P. vulgaris*, as well as transferred metabolites and mobile genes between *T. chinense* and its host.

According to currently available phytochemical investigations, *T. chinense* contains various compounds, with flavonoids being the main biologically active compounds responsible for its

265 pharmacological properties and therapeutic effectiveness [8]. In this study, *T. chinense* chimera
266 showed a higher proportion of downregulated flavonoids compared with individual *T. chinense*
267 (S2 Table). This could be a result of plant growth-defense trade-off where part of plant resources,
268 originally allocated to growth, were redirected towards defense mechanisms, thus obtaining
269 protective adaptation to environmental stresses. The active compounds of *P. vulgaris* mainly
270 include flavonoids, phenolic acids, and terpenoids [36,37]. After establishing a parasitic relationship,
271 most of flavonoids and terpenoids showed an upregulation trend (S3 Table). This result indicates
272 that parasitism promotes the accumulation of active compounds in *P. vulgaris*. These results
273 provide a basis for understanding the metabolic mechanisms of *T. chinense-P. vulgaris*
274 interactions, which will contribute to the quality control of *T. chinense*.

275 Phytohormones are important factors regulating plant growth and development [25]. By
276 analyzing the KEGG pathway, many DEGs in TH vs THC and P vs PC were found to be enriched
277 in plant hormone signal transduction (Fig. 4C and 4D). Emerging studies showed that the
278 formation of haustorium involves plant hormones such as auxin, cytokinins, and ethylene were
279 involved in the formation of haustorium [38]. Once successfully invaded, haustoria start forming
280 xylem bridges that connect between the host and parasite xylems to initialize material transfer.
281 Xylem bridge formation is supported by auxin flow generated by several PIN family auxin efflux
282 carriers and AUX1/LAX influx carriers genes expressed within invading haustoria [39].
283 Haustorium-inducing factors (HIFs) trigger the expression of an auxin biosynthesis gene in root
284 epidermal cells at the haustoria formation sites. This process leads to cell division and expansion,
285 resulting in the formation of a semi-spherical pre- or early haustorium structure [40]. Therefore, the
286 auxin biosynthesis/signaling-related genes were highly abundant in *T. chinense* haustoria [34].

287 Furthermore, the auxin response could be one of the shared mechanisms in haustoria formation
288 among parasitic plants [41]. In the present study, the levels of auxins such as indole, 3-
289 indolepropionic acid and 3-indoleacrylic acid decreased in *T. chinense* chimera (Table 1).
290 Similarly, a downtrend of auxin content was detected in *Cuscuta japonica* during its parasitization
291 [25]. The auxin pathway may play an important role in the host-parasite association [41]. Therefore,
292 auxin transport may participate in establishing the host-parasite association. JA is an ancient
293 regulator that controls the biosynthesis and/or transport of systemic signals, and it plays a crucial
294 role in the biosynthesis or transport of between-plant mobile signals [25]. Furthermore, the host JA
295 signaling plays a role in regulating the gene expression in the parasitizing *Cuscuta* [41]. In this
296 study, JA was upregulated in THC and PC (Table 1). However, the specific functions of JA in
297 parasitic plants remain unexplored. We speculate that the increased JA levels in *T. chinense*
298 chimera may be related to its defense mechanism against the host, as the chimera also
299 accumulating more JA. In short, the progression of haustorium organogenesis and the host-
300 parasite interaction is controlled by phytohormones. To understand how plants coordinate multiple
301 hormonal components in response to diverse developmental and environmental cues represents a
302 significant challenge for the future. In our study, the metabolic changes caused by *T. chinense*
303 parasitism were associated with phenylpropanoid biosynthesis, flavonoid biosynthesis, plant
304 hormone signal transduction, fructose and mannose metabolism, vitamin B6 metabolism and
305 photosynthesis-antenna proteins (Fig. 4C). The fructose and mannose metabolism pathway is
306 crucial for the success of parasitism [27]. In the case of *Orobanche aegyptiaca*, the host-induced
307 suppression of the mannose 6-phosphate reductase gene is concomitant with significant mannitol
308 decrease and increased tubercle mortality [42]. In plant-pathogen interaction, the pathogen secretes

309 mannitol as a buffer against oxidative stress, and the host plant activates mannitol dehydrogenase
310 to counter it [43]. In the study, the relatively high mannitol level in *P. vulgaris* chimera might be a
311 consequence of this host-parasite interaction (S3 Table).

312 Parasitic plants and their hosts are often phylogenetically very distant, and the haustoria
313 establish physical and physiological connections between the host and parasitic plants, thereby
314 dominating most of their interactions [6], making the host-parasite systems very suitable for the
315 identification of mobile substances. Secondary metabolites are essential for plant survival and are
316 typically biosynthesized in specific tissues and cell types before being transported to neighboring
317 cells or even to other tissues or other organs [44]. Some secondary metabolites in the host can be
318 transferred to the parasite plant [25]. We have identified 4 metabolites that were transferred from *P.*
319 *vulgaris* chimera to *T. chinense* chimera (Table 2). In this study, 2-ethylpyrazine was identified to
320 be the transferred metabolite from *T. chinense* chimera to *P. vulgaris* chimera (Table 2). Although
321 what effect 2-ethylpyrazine has on the parasitism relationship remains unknown, we speculate that
322 it may be a metabolite of *T. chinense* that attracts host plants and successfully colonizes them.
323 Actually, how parasitic plants accept secondary metabolites from their hosts and the ecological
324 impact of the translocated secondary metabolites in parasitic plants require further exploration [25].
325 In future experiments, we can apply 2-ethylpyrazine to *P. vulgaris* or other host plants of *T.*
326 *chinense* and observe whether *T. chinense* can colonize faster or promote its growth to verify the
327 role of 2-ethylpyrazine in contributing to establish parasitism relationship.

328 Compared to other host-pathogen systems [45], there were few reports on the interactions
329 between parasite plant-host [46]. An important aspect of the host-parasite interaction is the effect of
330 host's growth stage and environment on the mobile mRNAs expression [23]. The presence of

haustoria also facilitates the transfer of RNAs between parasitic plants and the host [47]. RNA-sequencing analysis has indicated the trafficking of thousands of mRNA species between hosts and *Cuscuta pentagona* [48]. There was also large-scale mobile mRNA between *Haloxylon ammodendron* and the parasitic plant *Cistanche deserticola* [46], and the mRNA abundance gradient is likely to be the determinant of mobility [25]. In this study, cross-species mRNA movement was identified between *T. chinense* and *P. vulgaris*, and 383 and 285 mobile mRNAs might be transferred from *T. chinense* and *P. vulgaris* to host and parasite through haustoria, respectively (S7 and S8 Table). However, these mobile transcripts need further investigation.

Conclusion

The study presents a comprehensive analysis of the metabolome and transcriptome of *T. chinense*, *P. vulgaris* and their chimeras. The identification of 5 transferred metabolites and 668 mobile genes exchanged between *T. chinense* and P. *vulgaris* underscores the complexity of the parasitic relationship, revealing a substantial inter-organismal transfer of resources and genetic information. The discovery of 56 metabolites and 189 genes related to haustoria formation further emphasizes the intricate biological processes underpinning the establishment of parasitism. The constructed gene regulatory network has pinpointed 18 genes that promote and one gene that inhibit haustoria formation, highlighting potential targets for further investigation into the mechanisms of parasitic plant development. The critical role of the fructose and mannose metabolism pathway in parasitism success is also emphasized. These findings indicate a strategic exploitation of host resources that are likely essential for the parasitic plant's survival and proliferation.

In conclusion, our results suggest that *T. chinense* engages in a sophisticated and dynamic

352 biological exchange with *P. vulgaris*, utilizing both metabolites and mobile mRNAs to facilitate
353 haustoria formation and successful parasitism. The elucidation of these complex interactions not
354 only expands our understanding of the molecular dialogues between parasitic and host plants but
355 also sets the stage for future explorations into controlling or harnessing these interactions for
356 agricultural and ecological benefit.

357 Materials and methods

358 Plant materials and sample collection

359 Five plants each of *T. chinense*, *P. vulgaris* and their commensal chimera were randomly selected
360 for sampling independent roots and chimeric roots, and the *T. chinense* chimera (THC) and *P.*
361 *vulgaris* chimera (PC) were sampled from the symbiont roots post parasitization. To minimize any
362 surface tissue contamination, the sampled roots or chimera with three biological replicates were
363 washed 1-2 times with PBS/RNase-free water, and frozen in liquid nitrogen and stored at −80°C
364 for the subsequent metabolomic, transcriptomic analysis.

365 Metabolome analysis

366 For the widely targeted metabolomic profiling, four type of root samples aforementioned were
367 freeze-dried by vacuum freeze-dryer (Scientz-100F). The freeze-dried sample was crushed using a
368 mixer mill (MM 400, Retsch) with a zirconia bead for 1.5 min at 30 Hz. Dissolve 50 mg of
369 lyophilized powder with 1.2 mL 70% methanol solution, vortex 30 seconds every 30 minutes for 6
370 times in total. Following centrifugation at 12000 rpm for 3 min, the extracts were filtrated (SCAA-
371 104, 0.22 μm pore size; ANPEL, Shanghai, China, http://www.anpel.com.cn/), then analyzed

using an UPLC-ESI-MS/MS system (UPLC, ExionLC™ AD，https://sciex.com.cn/; MS, Applied Biosystems 6500 Q TRAP, https://sciex.com.cn/) [49,50].

Based on the mass spectrometry data, metabolites were identified using the Metware Database (MWDB, Wuhan, China) (www.metware.cn) and quantified according to peak intensity. Both unsupervised principal component analysis (PCA) and orthogonal projections to latent structure-discriminant analysis (OPLS-DA) were used to observe the overall differences in metabolic profiles between groups to identify their significant differential metabolites. The quantification data of metabolites were normalized by unit variance scaling and used for the subsequent analysis (http://www.r-project.org/) [51].

Screening of differentially accumulated metabolites

To determine the metabolomic differences of *T. chinense* and its host post parasitization, the differentially accumulated metabolites (DAMs) in the TH vs THC and P vs PC groups were screened. Variable importance in projection (VIP) values were extracted from OPLS-DA results, those selected and metabolites with VIP ≥ 1 and absolute $|\log_2 \text{FoldChange}| \geq 1$ were defined as DAMs [52].

The DAMs were annotated using the KEGG Compound database (http://www.kegg.jp/kegg/compound/) and mapped to the KEGG Pathway database (http://www.kegg.jp/kegg/pathway.html) [53]. Then a KEGG pathway enrichment analysis was performed, and the significance was determined by hypergeometric test p-values ≤ 0.05.

RNA extraction, library construction, and sequencing

Total RNA was isolated using the Trizol Reagent [54] (Invitrogen Life Technologies, Shanghai, China). To ensure the RNA samples were integrated and DNA-free, agarose gelelectrophoresis was performed. RNA purity was then determined by a nanophotometer. Following that, a Qubit 2.0 Fluorometer and an Agilent 2100 BioAnalyzer were used to accurately measure RNA concentration and integrity, respectively. The qualified samples were processed with oligo (dT) beads to enrich the mRNA, which was broken into fragments and used as templates for the cDNA library. To qualify the cDNA library, the fluorometer was used for primary quantification and the bioanalyzer was then used to insert text size. The qualified library was sequenced using the Illumina HiSeq 6000 platform.

RNA-Seq analysis

Clean reads were obtained by eliminating low-quality reads and assembled using Trinity 2.8.5 software [55]. The transcripts were assembled and then clustered into unigenes. The method of fragments per kilobase of transcript per million fragments mapped (FPKM) was applied to calculate the expression levels of genes. DESeq2 [56] was used to identify differential expression genes (DEGs) based on the thresholds of the adjusted p-value padj < 0.05 and $|\log_2\text{FoldChange}| \geq 1$ [56]. Then DEGs were annotated by the NR, SwissProt, GO, KOG, Pfam, and KEGG databases. Finally, GO and KEGG pathway enrichment analysis were performed on DEGs to reveal functional modules and signal pathways of interest.

Integrated metabolomic and transcriptomic analysis

Based on the metabolite content and gene expression data, Pearson correlation tests were used to detect associations between gene expression and metabolite content. Correlations between DAMs and DEGs were filtered according to Pearson correlation coefficient (PCC) and *P*-value. Only the significant associations with $|PCC| > 0.80$ and $P\text{-value} < 0.05$ were selected for constructing network of metabolome and transcriptome, and the metabolite-gene relationships related to haustoria formation were visualized using Cytoscape (v3.9.0) [57].

Supporting information

S1 Table. Metabolites in the *T. chinense*, *P. vulgaris* and their chimeras.

S2 Table. The differentially accumulated metabolites (DAMs) in the *T. chinense* and *T. chinense* chimera.

S3 Table. The differentially accumulated metabolites (DAMs) in the *P. vulgaris* and *P. vulgaris* chimera.

S4 Table. The differentially accumulated metabolites (DAMs) related to haustoria formation.

S5 Table. The differentially expressed genes (DEGs) in the *T. chinense* and *T. chinense* chimera.

S6 Table. The differentially expressed genes (DEGs) in the *P. vulgaris* and *P. vulgaris* chimera.

S7 Table. Mobile 383 genes transferred from *T. chinense* chimera to *P. vulgaris* chimera.

S8 Table. Mobile 285 genes transferred from *P. vulgaris* chimera to *T. chinense* chimera.

S9 Table. The 189 genes related to haustoria formation.

431 **S10 Table. The correlation of haustoria formation related genes and metabolites.**

432 Acknowledgments

433 We would like to express our gratitude to the members of our laboratory for their suggestions and
434 guidance on the manuscript, and to Metware Biotechnology Co., Ltd. (Wuhan, China) for essential
435 technical support.

436 Author Contributions

437 Conceptualization: Mingpu Tan, Zengxu Xiang.

438 Data curation: Anping Ding, Mingpu Tan, Zengxu Xiang.

439 Investigation: Anping Ding, Ruifeng Wang.

440 Methodology: Anping Ding, Ruifeng Wang, Juan Liu, Wenna Meng.

441 Resources: Anping Ding, Ruifeng Wang, Zengxu Xiang.

442 Software: Anping Ding, Ruifeng Wang, Juan Liu, Wenna Meng.

443 Validation: Anping Ding, Ruifeng Wang.

444 Visualization: Anping Ding, Juan Liu, Wenna Meng, Gang Hu.

445 Writing – original draft: Anping Ding, Mingpu Tan.

446 Writing – review & editing: Mingpu Tan, Zengxu Xiang.

447 All authors have read and agreed to the published version of the manuscript.

448 Data availability

449 The RNA-seq raw data used in this study have been deposited in Sequence Read Archive (SRA)

450 database in NCBI under accession number PRJNA1054813

451 (https://www.ncbi.nlm.nih.gov/sra/PRJNA1054813, which will be released upon publication).

452 References

453 [1] Westwood JH, Yoder JI, Timko MP, DePamphilis CW. The evolution of parasitism in plants. Trends Plant Sci.
454 2010; 15(4):227-35. doi: 10.1016/j.tplants PMID: 20153240
455 [2] Goyet V, Wada S, Cui S, Wakatake T, Shirasu K, Montiel G, et al. Haustorium Inducing Factors for Parasitic
456 *Orobanchaceae*. Front Plant Sci. 2019; 10:1056. doi: 10.3389/fpls PMID: 31555315
457 [3] González-Fuente M. Parasitic plants are one step ahead: *Cuscuta* responds transcriptionally to different hosts.
458 Plant Physiol. 2023; 524. doi: 10.1093/plphys/kiad524 PMID: 37792723
459 [4] Atsatt PR. The Biology of Parasitic Flowering Plants. Job Kuij. 1970.
460 [5] Leso M, Kokla A, Feng M, Melnyk CW. Pectin modifications promote haustoria development in the parasitic
461 plant *Phtheirospermum japonicum*. Plant Physiol. 2023; 343. doi: 10.1093/plphys/kiad343 PMID: 37311199
462 [6] Yoshida S, Cui S, Ichihashi Y, Shirasu K. The Haustorium, a Specialized Invasive Organ in Parasitic Plants.
463 Annu Rev Plant Biol. 2016; 67(1):643-667. doi: 10.1146/annurev-arplant-043015-111702 PMID: 27128469
464 [7] Editorial Board of Flora of China. Flora of China. Science Press: Beijing, China, 1988; 76–80.
465 [8] Parveen Z, Deng Y, Saeed MK, Dai R, Ahamad W, Yu YH. Antiinflammatory and analgesic activities of
466 *Thesium chinense* Turcz extracts and its major flavonoids, kaempferol and kaempferol-3-O-glucoside.
467 Yakugaku Zasshi. 2007; 127(8):1275-9. doi: 10.1248/yakushi.127.1275 PMID: 17666881
468 [9] Liu ZZ, Ma JC, Deng P, Ren FC, Li N. Chemical Constituents of *Thesium chinense* Turcz and Their In Vitro
469 Antioxidant, Anti-Inflammatory and Cytotoxic Activities. Molecules. 2023; 28(6):2685. doi:
470 10.3390/molecules28062685 PMID: 36985657
471 [10] Yi Y , Jiang LZ , Xia XU, Wang L, Ying M. Comparion of Wild and Cultured *Thesium Chinense* Turcz on
472 Bacterio-stasis and Anti-inflammation. Pharmaceutical Biotechnology, 2006; 13(3):219. doi:10.1016/S0379-
473 4172(06)60071-1
474 [11] Wei J, Zhang C, Ma W, Ma J, Liu Z, Ren F, et al. Antibacterial Activity of *Thesium chinense* Turcz Extract
475 Against Bacteria Associated with Upper Respiratory Tract Infections. Infect Drug Resist. 2023; 16:5091-
476 5105. doi: 10.2147/IDR.S425398 PMID: 37576521
477 [12] Liu Y, Pan L, Qi K, et al. Sensitivity test of effective extracts from *Thesium chinense* to seven kinds of
478 bacteria. Guizhou Med. 2006; 6: 564-566.
479 [13] Liu C, Li XT, Cheng RR, Han ZZ, Yang L, Song ZC, et al. Anti-oral common pathogenic bacterial active
480 acetylenic acids from *Thesium chinense* Turcz. J Nat Med. 2018; 72(2):433-438. doi: 10.1007/s11418-018-
481 1180-3 PMID: 29435792
482 [14] Ding X, Zhang S, Ming L. Analgesic effect of Bairui buccal tablet on mice. J. Huaihai Med. 2001; 1:17-18.
483 [15] Shao L, Sun Y, Liang J, Li M, Li X. Decolorization affects the structural characteristics and antioxidant
484 activity of polysaccharides from *Thesium chinense* Turcz: Comparison of activated carbon and hydrogen
485 peroxide decolorization. Int J Biol Macromol. 2020; 155:1084-1091. doi: 10.1016/j.ijbiomac.2019.11.074
486 PMID: 31715240
487 [16] Xuan WD, Tang DH, Bian J, Shui-Gen HU, Jiang-Feng HU, Fan ZP. Therapeutic effects of *Thesium chinense*
488 on adriamycin-induced nephropathy rats. J Pharm Pract. 2012.

[17] Chen P, Chen X, Wu C, Meng Y, Cao J. Research progress on the development and utilization of *Thesium chinense* Turcz. Chin Wild Plant Resour. 2020; 39(06): 48-52.

[18] Li D, Li J, Yuan Y, Zhou J, Xiao Q, Yang T, et al. Risk factors and prognosis of acute lactation mastitis developing into a breast abscess: A retrospective longitudinal study in China. PLoS One. 2022; 17(9):e0273967. doi: 10.1371/journal.pone.0273967 PMID: 36048839

[19] Li GH, Fang KL, Yang K, Cheng XP, Wang XN, Shen T, et al. *Thesium chinense* Turcz.: An ethnomedical, phytochemical and pharmacological review. J Ethnopharmacol. 2021; 273:113950. doi: 10.1016/j.jep.2021.113950 PMID: 33610713

[20] Suetsugu K, Kawakita A, Kato M. Host range and selectivity of the hemiparasitic plant *Thesium chinense* (Santalaceae). Ann Bot. 2008; 102(1):49-55. doi: 10.1093/aob/mcn065 PMID: 18492736

[21] Pan J, Wang H, Chen Y. *Prunella vulgaris* L. A Review of its Ethnopharmacology, Phytochemistry, Quality Control and Pharmacological Effects. Front Pharmacol. 2022;13:903171. doi: 10.3389/fphar.2022.903171 PMID: 35814234

[22] David-Schwartz R, Runo S, Townsley B, Machuka J, Sinha N. Long-distance transport of mRNA via parenchyma cells and phloem across the host-parasite junction in *Cuscuta*. New Phytol. 2008; 179(4):1133-1141. doi: 10.1111/j.1469-8137 PMID: 18631294

[23] Roney JK, Khatibi PA, Westwood JH. Cross-species translocation of mRNA from host plants into the parasitic plant dodder. Plant Physiol. 2007; 143(2):1037-43. doi: 10.1104/pp.106.088369 PMID: 17189329

[24] LeBlanc M, Kim G, Patel B, Stromberg V, Westwood J. Quantification of tomato and *Arabidopsis* mobile RNAs trafficking into the parasitic plant *Cuscuta pentagona*. New Phytol. 2013; 200(4):1225-33. doi: 10.1111/nph.12439 PMID: 23914903

[25] Shen G, Zhang J, Lei Y, Xu Y, Wu J. Between-Plant Signaling. Annu Rev Plant Biol. 2023; 74:367-386. doi: 10.1146/annurev-arplant-070122-015430 PMID: 36626804

[26] Saucet SB, Shirasu K. Molecular Parasitic Plant-Host Interactions. PLoS Pathog. 2016; 12(12):e1005978. doi: 10.1371/journal.ppat.1005978 PMID: 27977782

[27] Feng R, Wei H, Xu R, Liu S, Wei J, Guo K, et al. Combined Metabolome and Transcriptome Analysis Highlights the Host's Influence on *Cistanche deserticola* Metabolite Accumulation. Int J Mol Sci. 2023; 24(9):7968. doi: 10.3390/ijms24097968 PMID: 37175675

[28] Kim G, LeBlanc ML, Wafula EK, dePamphilis CW, Westwood JH. Plant science. Genomic-scale exchange of mRNA between a parasitic plant and its hosts. Science. 2014; 345(6198):808-11. doi: 10.1126/science.1253122 PMID: 25124438

[29] Liu N, Shen G, Xu Y, Liu H, Zhang J, Li S, et al. Extensive Inter-plant Protein Transfer between *Cuscuta Parasites* and Their Host Plants. Mol Plant. 2020; 13(4):573-585. doi: 10.1016/j.molp.2019.12.002 PMID: 31812691

[30] Zhang CC, Gao Z, Luo LN, Zhang ZX, Wang J, Lu FH, et al. Transcriptome analysis of seed embryo in dormancy and dormancy release state of *Thesium chinense*. Zhongguo Zhong Yao Za Zhi. 2020; 45(16):3837-3843. Chinese. doi: 10.19540/j.cnki.cjcmm.20200506.109 PMID: 32893578

[31] Shin C, Choi D, Shirasu K, Ichihashi Y, Hahn Y. A novel RNA virus, *Thesium chinense* closterovirus 1, identified by high-throughput RNA-sequencing of the parasitic plant *Thesium chinense*. Acta Virol. 2022; 66(3):206-215. doi: 10.4149/av_2022_302 PMID: 36029083

[32] Ma J, Wei J, Chen G, Yan X, Sun H, Li N. Extracts of *Thesium chinense* inhibit SARS-CoV-2 and inflammatio in vitro. Pharm Biol. 2023; 61(1):1446-1453. doi: 10.1080/13880209.2023.2253841 PMID: 37675874

[33] Suetsugu K, Kawakita A, Kato M. Host range and selectivity of the hemiparasitic plant *Thesium chinense*

(Santalaceae). Ann Bot. 2008; 102(1):49-55. doi: 10.1093/aob/mcn065 PMID: 18492736

[34] Ichihashi Y, Kusano M, Kobayashi M, Suetsugu K, Yoshida S, Wakatake T, et al. Transcriptomic and Metabolomic Reprogramming from Roots to Haustoria in the Parasitic Plant, *Thesium chinense*. Plant Cell Physiol. 2018; 59(4):724-733. doi: 10.1093/pcp/pcx200 PMID: 29281058

[35] Bouwmeester H, Li C, Thiombiano B, Rahimi M, Dong L. Adaptation of the parasitic plant lifecycle: germination is controlled by essential host signaling molecules. Plant Physiol. 2021; 185(4):1292-1308. doi: 10.1093/plphys/kiaa066 PMID: 33793901

[36] Zhang JH, Qiu JN, Wang L, Zhang S, Jiang YY. Research progress on chemical constituents and pharmacological effects of *Prunella vulgaris*. Chinese Traditional and Herbal Drugs. 2018; 49(14):3432-3440. doi:10.7501/j.issn.0253-2670.2018.14.033

[37] Zhang X, Shen T, Zhou X, Tang X, Gao R, Xu L, et al. Network pharmacology based virtual screening of active constituents of *Prunella vulgaris* L. and the molecular mechanism against breast cancer. Sci Rep. 2020; 10(1):15730. doi: 10.1038/s41598-020-72797-8 PMID: 32978480

[38] Cui S, Inaba S, Suzaki T, Yoshida S. Developing for nutrient uptake: Induced organogenesis in parasitic plants and root nodule symbiosis. Curr Opin Plant Biol. 2023; 76:102473. doi: 10.1016/j.pbi.2023.102473 PMID: 37826989.

[39] Wakatake T, Ogawa S, Yoshida S, Shirasu K. An auxin transport network underlies xylem bridge formation between the hemi-parasitic plant *Phtheirospermum japonicum* and host *Arabidopsis*. Development. 2020; 147(14):dev187781. doi: 10.1242/dev.187781 PMID: 32586973

[40] Ishida JK, Wakatake T, Yoshida S, Takebayashi Y, Kasahara H, Wafula E, et al. Local Auxin Biosynthesis Mediated by a YUCCA Flavin Monooxygenase Regulates Haustorium Development in the Parasitic Plant *Phtheirospermum japonicum*. Plant Cell. 2016; 28(8):1795-814. doi: 10.1105/tpc.16.00310 PMID: 27385817

[41] Ashapkin VV, Kutueva LI, Aleksandrushkina NI, Vanyushin BF, Teofanova DR, Zagorchev LI. Genomic and Epigenomic Mechanisms of the Interaction between Parasitic and Host Plants. Int J Mol Sci. 2023; 24(3):2647. doi: 10.3390/ijms24032647 PMID: 36768970

[42] Aly R, Cholakh H, Joel DM, Leibman D, Steinitz B, Zelcer A, et al. Gene silencing of mannose 6-phosphate reductase in the parasitic weed Orobanche aegyptiaca through the production of homologous dsRNA sequences in the host plant. Plant Biotechnol J. 2009; 7(6):487-98. doi: 10.1111/j.1467-7652.2009.00418.x PMID: 19490480

[43] Patel TK, Williamson JD. Mannitol in Plants, Fungi, and Plant-Fungal Interactions. Trends Plant Sci. 2016; 21(6):486-497. doi: 10.1016/j.tplants.2016.01.006 PMID: 26850794

[44] Yazaki K. Transporters of secondary metabolites. Curr Opin Plant Biol. 2005; 8(3):301-307. doi:10.1016/j.pbi.2005.03.011

[45] Rivera-Cuevas Y, Carruthers VB. The multifaceted interactions between pathogens and host ESCRT machinery. PLoS Pathog. 2023; 19(5):e1011344. doi: 10.1371/journal.ppat.1011344 PMID: 37141275

[46] Fan Y, Zhao Q, Duan H, Bi S, Hao X, Xu R, et al. Large-scale mRNA transfer between *Haloxylon ammodendron* (Chenopodiaceae) and herbaceous root holoparasite *Cistanche deserticola* (Orobanchaceae). iScience. 2022; 26(1):105880. doi: 10.1016/j.isci.2022.105880 PMID: 36686392

[47] Guo C, Qin L, Ma Y, Qin J. Integrated metabolomic and transcriptomic analyses of the parasitic plant *Cuscuta japonica* Choisy on host and non-host plants. BMC Plant Biol. 2022; 22(1):393. doi: 10.1186/s12870-022-03773-9 PMID: 35934696

[48] Kim G, LeBlanc ML, Wafula EK, dePamphilis CW, Westwood JH. Plant science. Genomic-scale exchange of mRNA between a parasitic plant and its hosts. Science. 2014; 345(6198):808-11. doi: 10.1126/science.1253122 PMID: 25124438

[49] Chen W, Gong L, Guo Z, Wang W, Zhang H, Liu X, et al. A novel integrated method for large-scale detection, identification, and quantification of widely targeted metabolites: application in the study of rice metabolomics. Mol Plant. 2013; 6(6):1769-80. doi: 10.1093/mp/sst080 PMID: 23702596

[50] Fraga CG, Clowers BH, Moore RJ, Zink EM. Signature-discovery approach for sample matching of a nerve-agent precursor using liquid chromatography-mass spectrometry, XCMS, and chemometrics. Anal Chem. 2010; 82(10):4165-73. doi: 10.1021/ac1003568 PMID: 20405949

[51] Chong J, Xia J. MetaboAnalystR: an R package for flexible and reproducible analysis of metabolomics data. Bioinformatics. 2018; 34(24):4313-4314. doi: 10.1093/bioinformatics/bty528 PMID: 29955821

[52] Thévenot EA, Roux A, Xu Y, Ezan E, Junot C. Analysis of the Human Adult Urinary Metabolome Variations with Age, Body Mass Index, and Gender by Implementing a Comprehensive Workflow for Univariate and OPLS Statistical Analyses. J Proteome Res. 2015; 14(8):3322-35. doi: 10.1021/acs.jproteome.5b00354 PMID: 26088811

[53] Ogata H, Goto S, Sato K, Fujibuchi W, Bono H, Kanehisa M. KEGG: Kyoto Encyclopedia of Genes and Genomes. Nucleic Acids Res. 2000; 27(1):29-34. doi: 10.1093/nar/27.1.29 PMID: 9847135

[54] Olson WJ, Martorelli Di Genova B, Gallego-Lopez G, Dawson AR, Stevenson D, Amador-Noguez D, et al. Dual metabolomic profiling uncovers Toxoplasma manipulation of the host metabolome and the discovery of a novel parasite metabolic capability. PLoS Pathog. 2020; 16(4):e1008432. doi: 10.1371/journal.ppat.1008432 PMID: 32255806

[55] Grabherr MG, Haas BJ, Yassour M, Levin JZ, Thompson DA, Amit I, et al. Full-length transcriptome assembly from RNA-Seq data without a reference genome. Nat Biotechnol. 2011; 29(7):644-52. doi: 10.1038/nbt.1883 PMID: 21572440

[56] Love MI, Huber W, Anders S. Moderated estimation of fold change and dispersion for RNA-seq data with DESeq2. Genome Biol. 2014; 15(12):550. doi: 10.1186/s13059-014-0550-8 PMID: 25516281

[57] Shannon P, Markiel A, Ozier O, Baliga NS, Wang JT, Ramage D, et al. Cytoscape: a software environment for integrated models of biomolecular interaction networks. Genome Res. 2003; 13(11):2498-504. doi: 10.1101/gr.1239303 PMID: 14597658

Fig. 1 Morphology of *T. chinense* and its host *P. vulgaris* chimeric root. A: *T. chinense* and its host *P. vulgaris*. B: *T. chinense* chimera is connected to its host *P. vulgaris* chimera through haustoria. C-D: Structure of *T. chinense* chimera, haustoria and *P. vulgaris* chimera. THC: *T. chinense* chimera. H: Haustorium. PC: *P. vulgaris* chimera.

Fig. 2 The metabolomic analysis of *T. chinense* and its host *P. vulgaris* post symbiosis. A: Heat map visualization of metabolites in *T. chinense*, *P. vulgaris* roots and their chimera. B: PCA analysis of metabolites in *T. chinense*, *P. vulgaris* roots and their chimera. C: Venn diagrams revealing the relationship of differentially accumulated metabolites (DAMs) in *T. chinense* chimera and its host *P. vulgaris* chimera. TH: *T. chinense*. THC: *T. chinense* chimera. PC: *P.*

613 *vulgaris* chimera. P: *P. vulgaris*.

614 **Fig. 3 The proportion of differentially accumulated metabolites (DAMs) category in *T.***

615 ***chinense* chimera and its host *P. vulgaris* chimera.** A: TH vs THC. B: P vs PC. TH: *T. chinense*.

616 THC: *T. chinense* chimera. PC: *P. vulgaris* chimera. P: *P. vulgaris*.

617 **Fig. 4 The enrichment analysis of DEGs based on GO terms and KEGG pathways.** A: GO

618 terms of DEGs in TH vs THC. B: GO terms of DEGs in P vs PC. C: KEGG pathway analysis of

619 DEGs in TH vs THC. D: KEGG pathway analysis of DEGs in P vs PC. TH: *T. chinense*. THC: *T.*

620 *chinense* chimera. PC: *P. vulgaris* chimera. P: *P. vulgaris*.

621 **Fig. 5 Venn diagrams showing common and unique sets of transcripts in *T. chinense* and its**

622 **host *P. vulgaris* following parasition.** TH: *T. chinense*. THC: *T. chinense* chimera. PC: *P.*

623 *vulgaris* chimera. P: *P. vulgaris*.

624 **Fig. 6 The network of metabolites and genes related to haustoria formation.** Genes in the

625 green ellipse. The upregulated genes in both THC and PC chimeras were in red font and the

626 downregulated in blue font. Metabolites downregulated in both THC and PC are in the pink

627 triangle and metabolites upregulated in both THC and PC are in the orange triangle. For the

628 connection between genes and metabolites, red lines indicate the positive correlation while blue

629 lines indicate the negative correlation. The altered pattern and annotation of haustoria formation

630 related metabolites or genes are given in S10 Table.